

Lattice Expansion in Nanocrystalline Niobium Thin Films

G. B. Thompson – The Ohio State University
et al.

Deposited 11/12/2018

Citation of published version:

Banerjee, R., et al. (2003): Lattice Expansion in Nanocrystalline Niobium Thin Films. *Applied Physics Letters*, 82(24).

DOI: <https://doi.org/10.1063/1.1582361>

Lattice expansion in nanocrystalline niobium thin films

R. Banerjee,^{a)} E. A. Sperling, G. B. Thompson, and H. L. Fraser

Center for the Accelerated Maturation of Materials, Department of Materials Science and Engineering, The Ohio State University, Columbus, Ohio 43210

S. Bose and P. Ayyub

Department of Condensed Matter Physics and Materials Science, Tata Institute of Fundamental Research, Mumbai 400005, India

(Received 7 February 2003; accepted 9 April 2003)

High-purity nanocrystalline niobium (Nb) thin films have been deposited using high-pressure magnetron sputter deposition. Increasing the pressure of the sputtering gas during deposition has systematically led to reduced crystallite sizes in these films. Based on x-ray and electron diffraction results, it is observed that the nanocrystalline Nb films exhibit a significantly large lattice expansion with reduction in crystallite size. There is however, no change in the bcc crystal structure on reduction in crystallite size to below 5 nm. The lattice expansion in nanocrystalline Nb has been simulated by employing a recently proposed model based on linear elasticity and by appropriately modifying it to incorporate a crystallite-size-dependent width of the grain boundary. © 2003 American Institute of Physics. [DOI: 10.1063/1.1582361]

The currently widespread interest in the broad area of nanomaterials is primarily due to the properties exhibited by these materials.^{1,2} A wide variety of processing techniques are being employed by research groups around the world to synthesize nanomaterials. These include mechanical milling and alloying,³⁻⁵ controlled devitrification of amorphous materials,⁶⁻⁸ inert gas condensation and subsequent compaction,⁸⁻¹⁰ and sputter deposition.^{11,12} From the structural viewpoint, nanocrystalline materials are often visualized as consisting of two components: the grain interior and a large volume fraction of grain boundary.¹ The grain boundary separates the interior of one grain from its adjacent one. With reduction in the average grain or crystallite size, there appears to be changes in the crystal lattice of nanocrystalline materials, as evidenced by reports in the literature.^{3,7,11} These include examples of lattice expansion,^{3,11} contraction,^{13,14} and distortion,⁷ with reduction in the crystallite size for different nanocrystalline materials. Furthermore, while there have been quite a few attempts at rationalizing the origin of lattice changes in nanocrystalline materials,^{11,15,16} there still appears to be a lack of a coherent framework for understanding such changes as a function of the crystallite size.

In a recent study, it has been reported that nanocrystalline niobium, prepared by high-energy ball-milling, exhibits a lattice expansion with decreasing grain size, eventually undergoing an allotropic phase transformation from bcc to fcc when the average crystallite size is reduced below ~10 nm.^{3,17} While this is a rather interesting observation, there appears to be some uncertainty regarding this phase transformation since earlier reports speculate the possible formation of the fcc NbN compound in ball-milled nanocrystalline Nb.⁵ Unfortunately, the presence of interstitial contaminants (O, N) introduced from the atmosphere as well as others introduced from the media used for milling (typically

hardened steel balls) in nanocrystalline ball-milled material can make it rather difficult to delineate the actual influence of crystallite size on structure and properties. Therefore, the current study focuses on the synthesis and structural characterization of high-purity nanocrystalline Nb thin films.

The nanocrystalline Nb thin films have been deposited using high-pressure magnetron sputtering. This technique has been developed rather recently and consequently has not yet been used extensively for synthesis of nanomaterials.¹² However, the technique appears to be a promising one, especially for the synthesis of high-purity nanocrystalline materials. The sputter deposition was carried out in a custom-built UHV chamber with a base pressure prior to sputtering $\sim 5 \times 10^{-8}$ Torr. All depositions were carried out on oxidized Si substrates which had a thick (~200-nm) thermally grown amorphous oxide on the surface. The only processing variable that was systematically altered was the pressure of Ar gas in the chamber during sputtering. The Ar pressure was varied from 2 to 100 mTorr. Films were deposited at pressures of 2, 10, 50, and 100 mTorr. All the films were deposited for a 1 h at a dc power of 200 W. The target used for the sputter deposition was a commercially purchased elemental Nb target of 99.99% purity. Prior to introduction into the sputtering chamber, the Ar gas was purified by passing it through a gettering furnace consisting of a Ti sponge maintained at a temperature of 1073 K. The as-deposited Nb films have been characterized using x-ray diffraction (XRD) and transmission electron microscopy (TEM). The XRD studies were carried out in a Scintag XDS 2000 diffractometer using Cu K α as the incident radiation, while the TEM studies were carried out in a FEI/Philips CM200 electron microscope operating at 200 kV. The electron diffraction studies have been carried out using a camera length of 700 mm in the TEM.

XRD patterns, in the Bragg reflection geometry, from four films deposited at different Ar pressures, are shown Fig. 1(a). The primary peak visible for all four Nb films can be consistently indexed as the {110} peak corresponding to the

^{a)}Author to whom correspondence should be addressed; electronic mail: banerjee.8@osu.edu

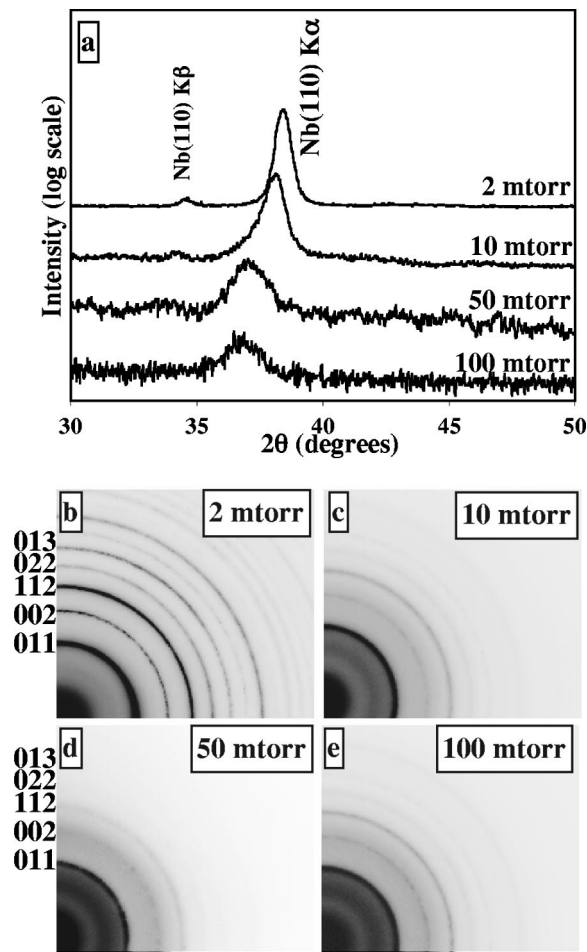


FIG. 1. (a) XRD patterns from the nanocrystalline Nb films deposited at different pressures of the sputtering gas. (b)–(e) Electron diffraction patterns in the plan-view geometry from the same Nb films.

bcc phase. As the Ar pressure increases, there is a systematic increase in the peak width full width at half-maximum. Since the peak width is inversely proportional to the XRD domain size (or crystallite size),¹⁸ the increase in peak width indicates a reduction in the mean crystallite size with increase in Ar pressure during sputtering. Based on the Debye–Scherrer broadening,¹⁸ the mean crystallite size has been calculated for these four films from the width of the {110} bcc Nb peak. In addition to the increasing width, there is also a systematic shift of the {110} peak to smaller 2θ values with increasing pressure of Ar [seen in Fig. 1(a)]. Such a shift indicates an increase in the interplanar spacing of {110} bcc planes. This suggests a possible lattice expansion or distortion in nanocrystalline Nb with reducing crystallite size. The XRD results were corroborated with electron diffraction results. Selected area electron diffraction patterns from the four nanocrystalline Nb films are shown in Figs. 1(b)–1(e). The rings in all the four patterns can be consistently indexed based on a single bcc phase, suggesting that there is no change or distortion in crystal structure with decreasing crystallite size. However, the lattice parameter of this bcc phase increases with increase in the pressure of sputtering gas or decrease in the crystallite size. The values of the lattice parameter measured from electron diffraction studies were in agreement with those measured from the {110} bcc peak in the XRD pattern. A plot of the bcc lattice parameter as a

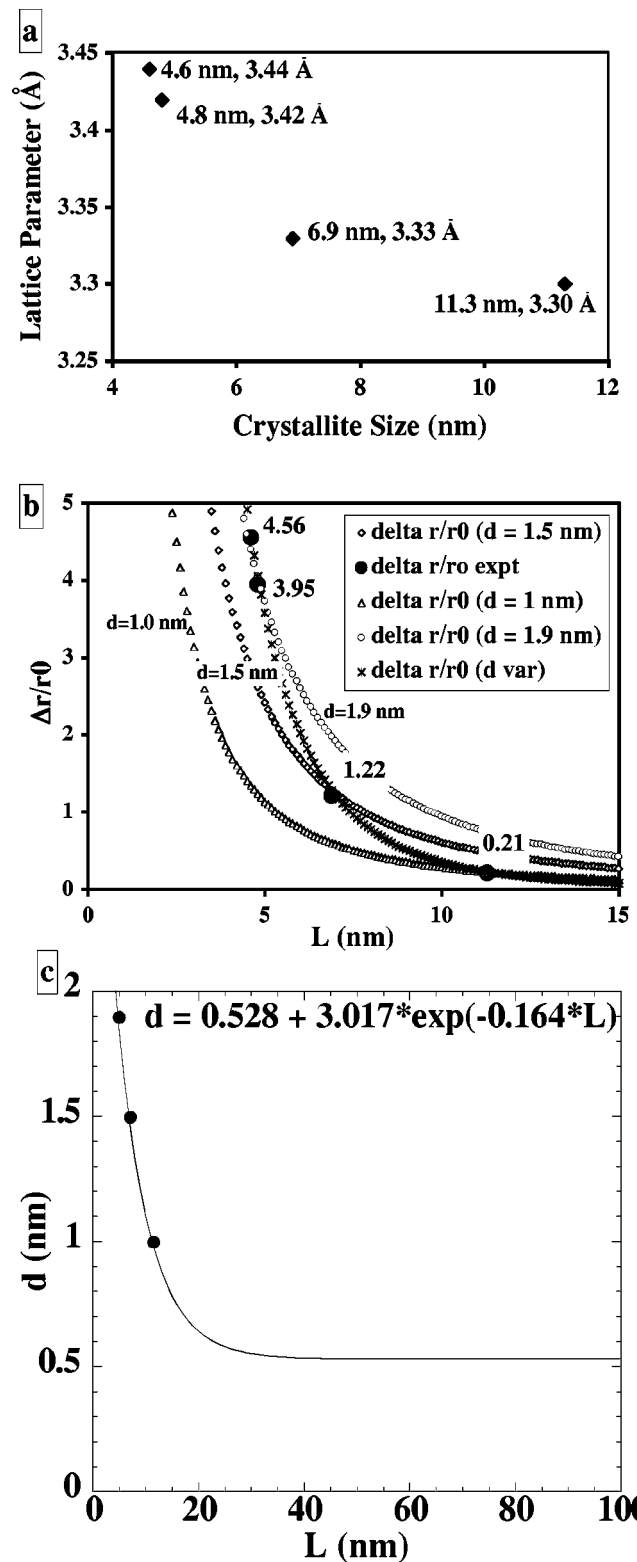


FIG. 2. (a) Experimentally observed variation in the lattice parameter of the bcc Nb phase in the nanocrystalline Nb films as a function of the crystallite size. (b) Predicted plots of the lattice expansion in nanocrystalline Nb ($\Delta r/r_0$) as a function of the crystallite size L for various widths d of the grain boundary and the experimentally determined values. (c) Plot of the variation of d as a function of L .

function of the crystallite size, measured from the Debye–Scherrer broadening of the {110} peak in the XRD pattern, is shown in Fig. 2(a). The increase in lattice parameter with decreasing crystallite size appears to exhibit a smooth, monotonic, nonlinear trend. No phase transformation from

bcc to fcc is observed in these nanocrystalline Nb films, even though the crystallite sizes for three of the films are substantially smaller than 10 nm. This suggests a possible influence of contaminants as well as the high degrees of strain introduced at very high strain rates during ball-milling, affecting the phase transformation reported in ball-milled nanocrystalline Nb for crystallite sizes below ~ 10 nm.^{3,17} In comparison, the nanocrystalline Nb thin films deposited by high-pressure magnetron sputtering are expected to have a relatively lower degree of strain.

The lattice expansion in nanocrystalline niobium has been rationalized using a recently proposed model based on linear elasticity.¹⁶ According to this model, the excess free volume of grain boundaries, arising from their highly disordered structure, results in a stress field within the grains causing an expansion of the lattice.¹⁶ By considering a nanometer-sized polycrystal model that consists of square-shaped crystallites with an orthogonal system of grain boundaries, the normalized lattice expansion can be expressed as follows:

$$\frac{\bar{r}}{r_0} = \frac{\bar{r} - r_0}{r_0} = \frac{1}{2L} \frac{d(d + 2a_0)}{d + a_0} (\sqrt[3]{1 + \Delta V} - 1), \quad (1)$$

where \bar{r} is the mean lattice parameter of the distorted crystallite, r_0 is the lattice parameter of the perfect crystallite, L is the mean grain or crystallite size, d is the mean width of the grain boundaries, a_0 is the nearest-neighbor separation of the perfect lattice, and ΔV is the excess free volume of the grain boundaries. It should be noted that the mean crystallite size L is smaller than the film thickness in all cases.

The excess free volume associated with the grain boundaries can be calculated using the following expression:¹⁷

$$\Delta V = \frac{(L + d/2)^2 - L^2}{L^2}. \quad (2)$$

In most prior calculations of the excess free volume, the width of the grain boundary has been assumed to be a constant ($d \approx 1$ nm), independent of the grain size.¹⁹ The predicted values of the normalized lattice expansion for nanocrystalline Nb, calculated using Eqs. (1) and (2), have been plotted as a function of grain size in Fig. 2(b). The graphs for three different values of the width of the grain boundary ($d = 1, 1.5,$ and 1.9 nm) have been plotted. The experimentally measured values of lattice expansion for the different grain sizes are also plotted in the same figure for comparison. Initially, the predicted curve for $d = 1$ nm was plotted for comparison with the experimental values. While the experimental value is in good agreement with the predicted value, with $d = 1$ nm at a grain size of 11.3 nm, the experimental values exceed the predictions ($d = 1$ nm) for smaller grain sizes. Subsequently, predicted curves have been plotted for $d = 1.5$ nm and $d = 1.9$ nm. These values of d have been selected based on the best fit of the experimental data for smaller crystallite sizes. The predicted value of lattice expansion for $d = 1.5$ nm agrees well with the experimental value for $L = 6.9$ nm, and for $L = 4.8$ and 4.6 nm there is good agreement with $d = 1.9$ nm. These results clearly indicate a possible change in the width d of the grain boundary. It appears that as the grain size decreases, the grain boundary

width increases. The experimental values of the grain size and the fitted values of the grain boundary width have been plotted in Fig. 2(c). Furthermore, the variation in d with L has been fitted using the exponential relationship:

$$d = 0.528 + 3.017 \exp(-0.164L). \quad (3)$$

Fitting the value of d to L via an exponential relationship appears to make physical sense since one would expect that as the grain size increased, the boundary width would tend towards a constant value for large grain sizes. From the curve fitting, the grain boundary width for Nb at large grain sizes (> 40 nm) is expected to be $d \approx 0.5$ nm. Using Eq. (3) for calculating d as a function of L in Eqs. (1) and (2), the normalized lattice expansion has been plotted as a function of L in Fig. 2(b). It should be noted that the three curves plotted previously based on Eqs. (1) and (2) assumed a constant value of d for each curve. This predicted curve is in excellent agreement with all the four experimental data points marked on the same figure.

To summarize, high-purity nanocrystalline Nb films with average crystallite sizes in the range of 5 to 12 nm have been deposited using the technique of high-pressure magnetron sputtering. The crystallite sizes in these films were inversely related to the pressure of Ar used for sputtering, which was varied from 2 to 100 mTorr. With reduction in crystallite size, there is a substantial expansion of the bcc lattice of nanocrystalline Nb. This lattice expansion does not appear to be accompanied with an allotropic phase transformation from bcc to fcc Nb, as reported earlier in the literature. The experimentally observed lattice expansion in nanocrystalline Nb is in excellent agreement with predictions afforded by a recently proposed model based on linear elasticity and suggests that the width of the grain boundary is likely to be a function of and not independent of the grain size in these nanocrystalline materials.

¹H. Gleiter, *Prog. Mater. Sci.* **33**, 223 (1989).

²R. W. Siegel, *Mater. Sci. Eng., A* **168**, 189 (1993).

³P. P. Chatterjee, S. K. Pabi, and I. Manna, *J. Appl. Phys.* **86**, 5912 (1999).

⁴E. Hellstern, L. Schultz, R. Bormann, and D. Lee, *Appl. Phys. Lett.* **53**, 1399 (1988).

⁵Z. Peng, C. Suryanarayana, and F. H. Froes, *Metall. Mater. Trans. A* **27**, 41 (1996).

⁶M. L. Sui and K. Lu, *Mater. Sci. Eng., A* **179/180**, 541 (1994).

⁷H. Y. Zhang, K. Lu, and Z. Q. Hu, *J. Phys.: Condens. Matter* **7**, 5327 (1995).

⁸D. H. Ping, D. X. Li, and H. Q. Ye, *J. Mater. Sci. Lett.* **14**, 1536 (1995).

⁹P. G. Sanders, J. A. Eastman, and J. R. Weertman, *Acta Math. Acad. Sci. Hung.* **45**, 4019 (1997).

¹⁰G. E. Fougere, L. Riester, M. Ferber, J. R. Weertman, and R. W. Siegel, *Mater. Sci. Eng., A* **204**, 1 (1995).

¹¹X. D. Liu, H. Y. Zhang, K. Lu, and Z. Q. Hu, *J. Phys.: Condens. Matter* **6**, L497 (1994).

¹²P. Taneja, R. Chandra, R. Banerjee, and P. Ayyub, *Scr. Mater.* **44**, 1915 (2001).

¹³F. W. C. Boswell, *Proc. Phys. Soc., London, Sect. A* **64**, 465 (1951).

¹⁴G. Pei-Yu, W. Kunth, H. Gleiter, and K. Weise, *Scr. Metall.* **22**, 683 (1988).

¹⁵M. Y. Gamarnik, *Phys. Status Solidi B* **178**, 59 (1993).

¹⁶W. Qin, Z. H. Chen, P. Y. Huang, and Y. H. Zhuang, *J. Alloys Compd.* **292**, 230 (1999).

¹⁷P. P. Chattopadhyay, P. M. G. Nambissan, S. K. Pabi, and I. Manna, *Phys. Rev. B* **63**, 054107 (2001).

¹⁸A. Guinier, *X-Ray Diffraction* (Freeman, San Francisco, 1963).

¹⁹R. W. Siegel, in *Processing of Metals and Alloys*, edited by R. W. Cahn, P. Hassen, and E. J. Krammer (VCH, Weinheim, Germany, 1991), p. 583.